THE JOURNAL OF BIOLOGICAL CHEMISTRY VOL. 287, NO. 9, pp. 6375–6386, February 24, 2012

Myeloperoxidase Targets Apolipoprotein A-I, the Major High Density Lipoprotein Protein, for Site-Specific Oxidation in Human Atherosclerotic Lesions*

Received for publication, December 22, 2011 Published, JBC Papers in Press, January 4, 2012, DOI 10.1074/jbc.M111.337345

Baohai Shao[‡1], **Subramaniam Pennathur**[§2], **and Jay W. Heinecke**[‡]

From the [‡]*Department of Medicine and Diabetes and Obesity Center of Excellence, University of Washington, Seattle, Washington 98195 and the* [§]*Department of Internal Medicine, University of Michigan, Ann Arbor, Michigan 48109*

Background: Oxidation of apolipoprotein A-I by myeloperoxidase has been proposed to deprive HDL of its cardioprotective effects.
Results: Tyrosine 192 is the major site of chlorination in apoA-I in both plasma and lesion HDL isolated from humans.
Conclusion: Chlorination of apolipoprotein A-I by myeloperoxidase may contribute to generation of a dysfunctional form of HDL *in vivo*.
Significance: Quantifying apolipoprotein A-I chlorination might help diagnose and perhaps treat human cardiovascular disease.

Oxidative damage by myeloperoxidase (MPO) has been proposed to deprive HDL of its cardioprotective effects. *In vitro* studies reveal that MPO chlorinates and nitrates specific tyrosine residues of apoA-I, the major HDL protein. After Tyr-192 is chlorinated, apoA-I is less able to promote cholesterol efflux by the ABCA1 pathway. To investigate the potential role of this pathway *in vivo*, we used tandem mass spectrometry with selected reaction monitoring to quantify the regiospecific oxidation of apoA-I. This approach demonstrated that Tyr-192 is the major chlorination site in apoA-I in both plasma and lesion HDL of humans. We also found that Tyr-192 is the major nitration site in apoA-I of circulating HDL but that Tyr-18 is the major site in lesion HDL. Levels of 3-nitrotyrosine strongly correlated with levels of 3-chlorotyrosine in lesion HDL, and Tyr-18 of apoA-I was the major nitration site in HDL exposed to MPO *in vitro*, suggesting that MPO is the major pathway for chlorination and nitration of HDL in human atherosclerotic tissue. These observations may have implications for treating cardiovascular disease, because recombinant apoA-I is under investigation as a therapeutic agent and mutant forms of apoA-I that resist oxidation might be more cardioprotective than the native form.

Many lines of evidence suggest that high density lipoprotein (HDL) normally protects against atherosclerosis by removing excess cholesterol from macrophages in the artery wall, a process termed reverse cholesterol transport (1–4). Lipid-free apolipoprotein A-I (apoA-I) promotes the efflux of macrophage plasma membrane cholesterol and phospholipids by an active process mediated by a transporter called ATP binding cassette transporter A1 (ABCA1)[3] (3, 5). Atherosclerosis in hypercholesterolemic mice increases markedly when myeloid cells lack ABCA1, whereas ABCA1 overexpression significantly reduced the development of atherosclerosis (6–10), indicating that the cell membrane transporter of myeloid cells plays a key role in reverse cholesterol transport in this animal model. Lecithin:cholesterol acyltransferase then converts free cholesterol to cholesteryl esters, an essential step in HDL maturation (11, 12). ABCG1, another ABC transporter expressed by macrophages, promotes cholesterol efflux to HDL (5, 13).

HDL has been proposed to lack cardioprotective effects or to be dysfunctional in subjects with atherosclerosis, but the underlying mechanisms are poorly understood (14–17). One possibility is that oxidative reactions change HDL composition and structure, preventing it from performing its normal functions.

Macrophages play a key role in lesion initiation and progression, raising the possibility that these inflammatory cells might be an important source of oxidants that damage HDL in the artery wall. One potential pathway involves reactive intermediates made by myeloperoxidase (MPO), a heme enzyme expressed at high levels by macrophages in the human artery wall (18). Indeed, when lipid-free apoA-I is oxidized by MPO *in vitro*, its ability to promote cellular cholesterol efflux by the ABCA1 pathway is impaired (19–21). Moreover, oxidation of lipid-associated apoA-I by MPO inhibits the protein ability to

* This work was supported, in whole or in part, by National Institutes of Health Grants R00HL091055, R01HL086798, R01HL085437, and R01HL077268. This work was also supported in part by the Proteomics Resource, University of Washington Grant UWPR95794.

[1] Supported by NHLBI, National Institutes of Health K99/R00 Award R00HL091055 and also by a Pilot and Feasibility Award from the University of Washington Diabetes Research Center (P30DK017047). To whom correspondence should be addressed: Box 358055, Division of Metabolism, Endocrinology, and Nutrition, Dept. of Medicine, University of Washington-South Lake Union, 815 Mercer St., Seattle, WA 98109. E-mail: bhshao@u.washington.edu.

[2] Supported by Doris Duke Foundation Clinical Scientist Development Award, the American College of Rheumatology within Our Reach Award, and by the Molecular Phenotyping Core of the Michigan Nutrition and Obesity Research Center (Grant DK089503).

[3] The abbreviations used are: ABCA1, ATP binding cassette transporter A1; ABCG1, ATP binding cassette transporter G1; apoA-I, apolipoprotein A-I; DTPA, diethylenetriaminepentaacetic acid; ESI, electrospray ionization; HDL_3, high-density lipoprotein-3; LC, liquid chromatography; MPO, myeloperoxidase; *m/z*, mass-to-charge ratio; $NO_2^{\bullet}$, NO_2 radical; SRM, selected reaction monitoring.

activate lecithin:cholesterol acyltransferase (22, 23). Also, HDL is also anti-inflammatory and inhibits lipid oxidation *in vivo* (14, 24), and those properties may contribute significantly to its ability to inhibit atherosclerosis.

MPO uses hydrogen peroxide (H_2O_2) for oxidative reactions in the extracellular milieu (25–27). The major end product at plasma concentrations of chloride ion (Cl^-) is generally thought to be hypochlorous acid (HOCl), a highly reactive oxidant that converts free and protein-bound tyrosine residues to 3-chlorotyrosine (28, 29). Studies of mice deficient in MPO demonstrate that 3-chlorotyrosine is a specific product of the enzyme *in vivo* (30). Another pathway for oxidizing artery wall proteins involves nitric oxide (NO) (31–33), which reacts rapidly with superoxide ($O_2^{\cdot-}$) to form peroxynitrite ($ONOO^-$), a reactive nitrogen species (34). Furthermore, oxidation of NO produces nitrite (NO_2^-), which reacts with H_2O_2 and MPO to generate nitrogen dioxide radical ($NO_2^{\cdot}$), a potent nitrating intermediate (35–37). $ONOO^-$ and $NO_2^{\cdot}$ generate 3-nitrotyrosine when they react with tyrosine residues (35, 36, 38, 39). Both pathways appear to contribute to the formation of reactive nitrogen species because MPO deficiency only partially abrogates the generation of 3-nitrotyrosine *in vivo* (36). Such reactive nitrogen species might promote inflammation by nitrating lipoproteins and other artery wall proteins.

In vitro studies reveal that MPO chlorinates and nitrates specific tyrosine residues of apoA-I (19, 20). Chlorination of tyrosine residue 192 (Tyr-192) of apoA-I strongly associates with loss of ABCA1 activity (19, 20). Moreover, we observed near normal cholesterol efflux activity when Tyr-192 of apoA-I was mutated to phenylalanine (Phe) and methionine sulfoxide residues in the oxidized protein were reduced enzymatically to methionine (40). These observations indicate that neither Tyr-192 chlorination nor methionine oxidation alone deprives apoA-I of its cholesterol efflux activity. However, a combination of the two, perhaps together with other structural changes, almost completely destroys that activity. Oxidation of apoA-I by MPO may be a regioselective pathway for generating dysfunctional HDL in the artery wall because HDL isolated from atherosclerotic lesions of humans contains much higher levels of 3-chlorotyrosine and 3-nitrotyrosine than does plasma HDL (19, 21, 41).

Two models have been proposed to explain the site-specific chlorination of Tyr-192 in apoA-I by MPO. One potential mechanism involves chloramine formation at Lys-195, which in turn promotes chlorination of Tyr-192 (42). A different model proposes that MPO binds directly to the region of apoA-I that contains Tyr-192 (21). To distinguish between these two models, we used site-directed mutagenesis to engineer a series of mutations in the lysine and methionine residues of human apoA-I (40). Studies with those mutations provided strong evidence that Y*XX*K can direct the regiospecific chlorination of tyrosine residues.

Mass spectrometric (MS) analyses have detected nitrated and chlorinated Tyr residues in peptides derived from apoA-I of HDL isolated from atherosclerotic lesions (43). However, those studies were not quantitative because they measured the ion current of specific peptides, and different peptides from the same protein can exhibit a wide range of ionization efficiencies and hence relative ion currents (44). No attempt has been made to quantitatively assess the regiospecific modification of all seven Tyr residues in apoA-I isolated from lesion or plasma HDL, and the overall susceptibility to *in vivo* oxidation of different residues in apoA-I remains unclear.

Selected reaction monitoring (SRM) is a quantitative and sensitive MS technique for detecting peptides and post-translational modifications of peptides (45, 46). In SRM, peptides of interest are fragmented into ions that are selectively monitored by MS/MS (45, 46). The *m*/*z* values of a precursor and product ion are referred to as an SRM "transition." This technique greatly reduces chemical noise, markedly improving the signal to noise ratio (45, 46). Furthermore, the instrument duty cycle is almost entirely used to monitor specific ions of interest. LC-MS/MS with SRM is thus capable of extraordinary sensitivity (45, 46).

It is important to determine the mechanism(s) and specific sites of chlorination and nitration of apoA-I *in vivo* because MPO (15, 47, 48) and recombinant apoA-I (50–52) represent potential therapeutic interventions in humans, and mutant forms of the protein that are resistant to oxidation might be more cardioprotective than the native form. In the current studies, we used SRM to globally assess levels of chlorinated and nitrated Tyr residues in apoA-I isolated from HDL from human plasma and atherosclerotic tissue. To further increase its power and obtain a quantitative measure of site-specific oxidation, we generated isotope-labeled [^{15}N]apoA-I protein for use as an the internal standard (22, 53). This quantitative analytical approach demonstrated that Tyr-192 is the major chlorination site in apoA-I of HDL isolated from human plasma and atherosclerotic tissue. We also tested the role of MPO binding in promoting the site-specific chlorination of apoA-I *in vitro*. Our observations support the proposal that chlorination of apoA-I by MPO may generate a dysfunctional form of HDL *in vivo*.

EXPERIMENTAL PROCEDURES

Materials—MPO (donor:hydrogen peroxide, oxidoreductase, EC 1.11.1.7) was isolated from human neutrophils by lectin affinity and size exclusion chromatographies (54) and stored at −20 °C. Enzyme concentration ($A_{430}/A_{280}>0.8$) was determined spectrophotometrically (ϵ_{430} = 178 $mM^{-1}cm^{-1}$) (55). Sodium hypochlorite (NaOCl), trifluoroacetic acid (TFA), acetonitrile (CH_3CN), and methanol were obtained from Fisher Scientific. [^{15}N]apoA-I was prepared by growing bacteria stably expressing human apoA-I in minimal medium supplemented with [^{15}N]nitrite (56). All organic solvents were HPLC grade. Unless otherwise indicated, all other materials were purchased from Sigma.

Isolation of HDL_3 and ApoA-I—Plasma was prepared from EDTA-anticoagulated blood of healthy adult subjects who had fasted overnight. HDL_3 (density 1.125–1.210 g/ml) was isolated from plasma by sequential ultracentrifugation and depleted of apolipoproteins E and B100 by heparin-agarose chromatography (57). ApoA-I was purified from HDL by ion-exchange chromatography (57). For biochemical procedures, protein concentration of apoA-I and HDL was determined using the Lowry assay (Bio-Rad) with albumin as the standard. The Human Studies committees at the University of Washington School of

Medicine and University of Michigan approved all protocols involving human material.

Isolation of Total HDL from Lesion or Plasma—Atherosclerotic tissue was harvested at endarterectomy, snap-frozen, and stored frozen at −80 °C until analysis. Lesions from a single individual (~0.5 g wet weight) were mixed with dry ice and pulverized in a stainless steel mortar and pestle (19). Plasma was obtained from overnight-fasted, apparently healthy adult subjects of either sex and any race that were over 21 years of age. Total lesion or plasma HDL (density 1.063–1.210 g/ml) was isolated from extracts of tissue powder or from plasma by ultracentrifugation (19, 41, 58) using buffers supplemented with 100 μM diethylenetriaminepentaacetic acid (DTPA, a chelator of redox active metal ions; ref (59)), 100 μM butylated hydroxytoluene (a lipid-soluble inhibitor of lipid peroxidation (60)), and a protease inhibitor mixture (Sigma). ApoA-I was detected by immunoblotting using a rabbit IgG polyclonal antibody to human apoA-I (Calbiochem) followed by a horseradish peroxidase-conjugated goat anti-rabbit IgG. Detection was enhanced by chemiluminescence.

Oxidation of apoA-I and HDL—Oxidative reactions were carried out at 37 °C for 1 h in phosphate buffer (20 mM sodium phosphate, 100 μM DTPA, pH 7.4) containing 5 μM apoA-I or 20 μM synthetic peptide LAEYHAK (GenScript USA Inc. Piscataway, NJ) (20). For the MPO-H_2O_2-chloride system, the reaction mixture was supplemented with 100 nM MPO and 100 mM NaCl. For the MPO-H_2O_2-nitrite system, it was supplemented with 100 nM MPO and 200 μM nitrite. Reactions were initiated by adding oxidant and terminated by adding methionine (20:1, Met/oxidant, mol/mol). $ONOO^-$ was synthesized from nitrite and H_2O_2 under acidic conditions; peroxynitrous acid was stabilized by rapidly quenching the reaction with excess sodium hydroxide (34). Concentrations of $ONOO^-$, HOCl, and H_2O_2 were determined spectrophotometrically ($\epsilon_{302} = 1670\ M^{-1}\ cm^{-1}$, $\epsilon_{292} = 350\ M^{-1}\ cm^{-1}$, and $\epsilon_{240} = 39.4\ M^{-1}cm^{-1}$, respectively) (34, 61).

Liquid Chromatography-Electrospray Ionization Tandem Mass Spectrometry (LC-MS/MS)—LC-MS/MS analyses of native or oxidized synthetic peptide LAEYHAK were performed on a Finnigan LTQ linear ion trap mass spectrometer (Thermo Electron Corp., San Jose, CA) coupled to a Paradigm MS4 LC system (Michrom BioResources, Inc.) as previous described (62). Peptides were separated at a flow rate of 1.0 μl/min on a Magic C18 AQ column (150 × 0.15 mm, 5 μm 200A, Michrom BioResources, Inc.) using solvent A (0.1% formic acid, 1% CH_3CN in water) and solvent B (0.1% formic acid in 90% CH_3CN). Peptides were eluted using a linear gradient of 0–40% solvent B over 40 min. A spray voltage of 1.8 kV was applied, and the heated metal capillary was maintained at 200 °C. The analyses were performed in the positive ion mode with a mass range of 200–2000 Da. MS/MS spectra were obtained using data-dependent acquisition. The normalized collision energy was 35%.

HPLC Analysis of Synthetic Peptide—Native or oxidized synthetic peptide LAEYHAK was separated at a flow rate of 0.3 ml/min on a reverse-phase column (Discovery BIO Wide Pore C18, 2.1 × 100 mm, 3 μm) using an Agilent 1200 Series HPLC system (Santa Clara, CA) with UV detection at 280 nm. The peptides were eluted using a gradient of solvent A (0.1% HCOOH and 1% acetonitrile in H_2O) and solvent B (0.1% HCOOH 10% H_2O in acetonitrile). Solvent B was increased from 0 to 40% over 30 min.

Proteolytic Digestion of Proteins—Total HDL, HDL_3, or apoA-I was incubated overnight at 37 °C with 20:1 (w/w, based on the Lowry assay) of sequencing grade modified trypsin (Promega) or endoproteinase Glu-C (from *Staphylococcus aureus* V8, Roche Applied Science) in 50 mM NH_4HCO_3, pH 7.8 (20, 22, 63, 64). For HDL, proteins were reduced with dithiothreitol and alkylated with iodoacetamide before digestion. Digestion was halted by acidifying the reaction mixture, pH 2–3, with trifluoroacetic acid. Proteolytic digests were desalted with a C18 ZipTip (Millipore) before MS analysis.

SRM—Samples were analyzed by nano-LC-MS/MS on a Thermo TSQ Quantum Access coupled to a Waters nanoACQUITY UltraPerformance liquid chromatography (nano-LC) system. The analytical column (15 cm × 75 μm inner diameter) was packed in-house with C-18 Magic C18 reverse-phase resin (5 μm; Michrom Bioresources). To detect the hydrophilic peptide containing Tyr-192 (LAE*Y*HAK) that was derived from tryptic digests of apoA-I, samples (0.5 μg of HDL protein) were directly loaded onto the analytical column. Peptides were eluted from the column at a flow rate of 0.35 μl/min using solvent A (0.1% formic acid in water) and solvent B (0.1% formic acid in acetonitrile). To load the peptides and wash the column, solvent B was kept at 0% for 40 min during sample loading. Solvent B was then increased to 35% over 50 min to elute the peptides. The instrument was operated in the positive ion mode. MS source parameters were as follows: spray voltage, 2.2 kV; capillary temperature, 235 °C; scan mode, SRM; scan width (m/z), 0.002; scan time, 0.05 s; Q1 peak width (full width at half-maximum), 0.70; skimmer offset, 5 V; Q2 collision gas pressure, 1.3 millitorr. Argon (Polar Cryogenics) was the collision gas. Four SRM transitions of each peptide in apoA-I that contained native or oxidized Tyr residues were chosen for quantitative analysis based on the tandem MS spectrum obtained with the TSQ instrument (Tables 1 and 2). SRM data were analyzed with Skyline, an open source program (65), to obtain the peak area of each transition and the total peak area of four transitions for each native and isotope-labeled peptide.

Quantification of Oxidized Products in Vitro—Chlorinated or nitrated tyrosine containing peptides in proteolytic digests of native or oxidized HDL_3 or lipid-free apoA-I were detected and quantified using reconstructed ion chromatograms of precursor and product peptides. Product yield (%) = peak area of product ion/sum (peak area of precursor ion + peak areas of product ions) × 100 (64). For SRM, the total peak area of four selected transitions was used to quantify the product yield of chlorinated or nitrated tyrosine residues. The same method was applied to the quantification of peptides using HPLC with monitoring of UV adsorption, the peak areas of the peptides, and the extinction coefficients of Tyr ($\epsilon_{280} = 1368\ M^{-1}cm^{-1}$ (66), chloro-Tyr ($\epsilon_{280} = 1879\ M^{-1}cm^{-1}$ (66), and nitro-Tyr ($\epsilon_{280} = 4300\ M^{-1}cm^{-1}$ (67).

Quantification of Oxidized apoA-I by SRM with Isotope Dilution—Oxidized apoA-I peptides of digests of plasma or lesion HDL were quantified by isotope dilution using

TABLE 1

SRM transitions for quantifying peptides of apoA-I in human HDL that contain chlorinated and nitrated tyrosine residues

Unlabeled peptides were derived from tryptic digests.

Residues	Peptide sequence	Precursor ion, *m*/*z* (Q1)	Product ions, *m*/*z* (Q3)
13–23	DLATV**Y**VDVLK	618.35 (+2)	229.12 (b_2), 736.42 (y_6), 835.49 (y_7), 936.54 (y_8)
28–40	D**Y**VSQFEGSALGK	700.84 (+2)	279.10 (b_2), 661.35 (y_7), 808.42 (y_8), 1023.51 (y_{10})
97–106	VQP**Y**LDDFQK	626.81 (+2)	228.13 (b_2), 765.38 (y_6), 928.44 (y_7), 1025.49 (y_8)
108–116	WQEEMEL**Y**R	642.29 (+2)	315.15 (b_2), 711.35 (y_5), 840.39 (y_6), 969.43 (y_7)
114–125	L**Y**RQKVEPLRAE[a]	501.29 (+3)	459.26 (b_7^{+2}), 585.34 (y_5), 714.38 (y_6), 694.88 (y_{11}^{+2})
161–171	THLAP**Y**SDELR	651.33 (+2)	352.20 (b_3), 879.42 (y_7), 950.46 (y_8), 1063.54 (y_9)
189–195	LAE**Y**AK	416.22 (+2)	185.13 (b_2), 518.27 (y_4), 647.31 (y_5), 718.35 (y_6)
227–238	VSFLSALEE**Y**TK	693.86 (+2)	334.18 (b_3), 782.39 (y_6), 853.43 (y_7), 940.46 (y_8)

[a] Peptides derived from Glu-C digests.

TABLE 2

Retention times (RT) of peptides of apoA-I in human HDL that contain chlorinated and nitrated tyrosine residues

Unlabeled peptides derived from tryptic digests.

Residues	Peptide	Precursor	RT	Chlorinated	RT	Nitrated	RT
		m/*z*	*min*	*m*/*z*	*min*	*m*/*z*	*min*
13–23	DLATV**Y**VDVLK	618.35 (+2)	85.6	635.35 (+2)	89.5	640.85 (+2)	92.7
28–40	D**Y**VSQFEGSALGK	700.84 (+2)	80.4	717.84 (+2)	83.1	723.34 (+2)	83.6
97–106	VQP**Y**LDDFQK	626.81 (+2)	74.5	643.81 (+2)	78.1	649.31 (+2)	79.0
108–116	WQEEMEL**Y**R	642.29 (+2)	76.6			664.79 (+2)	81.7
114–125	L**Y**RQKVEPLRAE[a]	501.29 (+3)	63.8	512.62 (+3)	66.5	516.28 (+3)	67.0
161–171	THLAP**Y**SDELR	651.33 (+2)	68.5	668.33 (+2)	71.8	673.83 (+2)	73.6
189–195	LAE**Y**HAK	416.22 (+2)	58.1	433.22 (+2)	61.5	438.72 (+2)	62.6
227–238	VSFLSALEE**Y**TK	693.86 (+2)	91.2	710.86 (+2)	95.9	716.36 (+2)	97.9

[a] Peptides derived from Glu-C digests.

[^{15}N]apoA-I as the internal standard (22, 53, 58). A dialyzed mixture of HOCl-chlorinated and peroxynitrite-nitrated [^{15}N]apoA-I (0.15 μg) was added to 10 μg of HDL before digestion. Chlorinated and nitrated tyrosine-containing peptides derived from apoA-I and [^{15}N]apoA-I were quantified by SRM. Levels of chlorinated and nitrated Tyr residues were derived from the ratios of oxidized peptide to precursor peptide of oxidized-[^{15}N]peptide and [^{15}N]peptide, respectively, using the following relationship: (μmol/mol Tyr) = 10^6 × [(amount of ^{15}N-labeled modified peptide) × (peak area of modified peptide from endogenous apoA-I)/(peak area of modified peptide from ox-[^{15}N]apoA-I)]/[(amount of ^{15}N-labeled precursor peptide) × (peak area of precursor peptide from endogenous apoA-I)/(peak area of precursor peptide from [^{15}N]apoA-I)]. The amount of modified ^{15}N-labeled peptide was obtained as described above. Levels of 3-chlorotyrosine or 3-nitrotyrosine in apoA-I were calculated as the sum of individual levels of 3-chlorotyrosine or 3-nitrotyrosine in apoA-I divided by 7 (apoA-I contains 7 Tyr residues).

Statistical Analysis—Unless otherwise indicated, results represent the means and S.D. and are representative of at least two independent experiments.

RESULTS

SRM Is Sensitive Method for Quantifying Regiospecific Oxidation of ApoA-I—To determine the optimal transitions for quantifying apoA-I and its oxidation products by SRM, we first obtained LC-ESI-MS and MS/MS spectra of each peptide that contained a Tyr residue. We then selected the four most abundant product ions for quantitative analysis (Table 1). To maximize analytical sensitivity and quantify site-specific modifications of apoA-I, we used a triple quadrupole mass spectrometer coupled to a nano-LC system to detect peptides and included HOCl- and peroxynitrite-oxidized [^{15}N]apoA-I in the digestion reaction as an internal standard. This approach detected all seven tyrosine-containing peptides and the corresponding chlorinated and nitrated products. Fig. 1 provides ion chromatograms of the peptides containing Tyr-192 and chlorinated Tyr-192 (ClY^{192}). *Panel A* shows the native and chlorinated peptides, and *Panel B* shows the product ions derived from the precursor peptides. The ^{15}N-labeled peptides eluted from the column with virtually the same retention time as the unlabeled peptides (Fig. 1A), but the ions derived from the ^{15}N-labeled peptides exhibited the anticipated increases in *m*/*z* (Fig. 1*B*). Importantly, the MS/MS spectra of the unlabeled and ^{15}N-lablled peptides that contained tyrosine were identical, indicating that the transitions selected for the analysis should provide both identification and quantitative information.

To confirm that our SRM analysis was quantitative, we used the synthetic peptide LAEYHAK (which mimics the tryptic peptide of apoA-I that contains Tyr-192) and determined the product yields of 3-chlorotyrosine and 3-nitrotryosine by SRM or HPLC with monitoring of A_{280}. When peptide (20 μM) was exposed to H_2O_2 (20 μM) using the MPO-chloride or MPO-nitrite system, the product yields of chlorinated or nitrated peptide detected by SRM and HPLC were almost identical (chloro-Tyr, 16 and 14%, respectively; nitro-Tyr, 41 and 38%, respectively). Similar results were observed when we quantified the levels of chlorinated and nitrated Tyr-192 in tryptic digests of oxidized apoA-I. These observations support the proposal that our SRM approach accurately quantifies chlorinated and nitrated residues in apoA-I.

The *in vivo* levels of oxidized apoA-I are likely to be low. We therefore determined the ability of SRM to quantify the levels of chlorinated and nitrated Tyr residues in apoA-I over a wide range of concentrations. Serial dilutions of a tryptic digest of a mixture of chlorinated and nitrated [^{15}N]apoA-I were added to a fixed amount of a tryptic digest of HDL (from 1:2 to 1:1000, [^{15}N]apoA-I/HDL protein, μg/μg). We then used SRM to

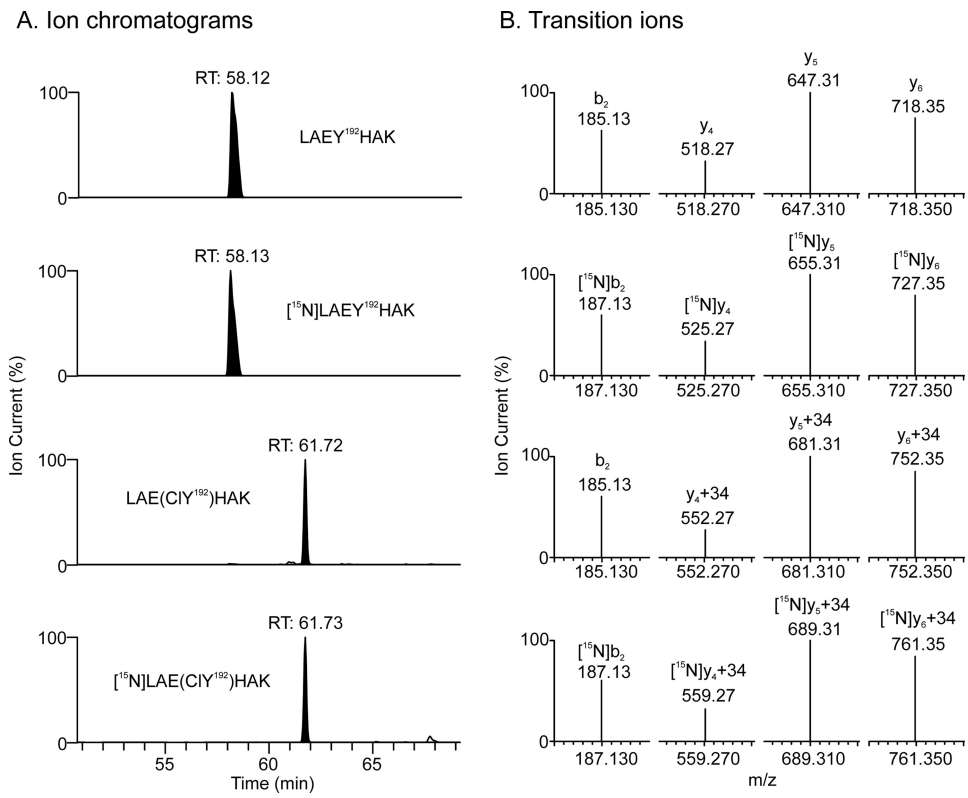

FIGURE 1. **Detection of chlorinated Tyr-192 peptide in HDL supplemented with plasma apoA-I and isotope-labeled apoA-I that had been oxidized by HOCl.** Lipid-free apoA-I (3.5 μM) and [^{15}N]apoA-I (3.5 μM) were exposed to 175 μM HOCl (50:1, mol/mol, HOCl:apoA-I) for 60 min at 37 °C in phosphate buffer (20 mM sodium phosphate, 100 μM DTPA, pH 7.4). After the reactive intermediates were quenched with L-methionine (5 mM), the reaction mixture was dialyzed against 10 mM sodium phosphate buffer, pH 7.4. Dialyzed HOCl-modified apoA-I (0.2 μg) and dialyzed HOCl-modified [^{15}N]apoA-I (0.2 μg) were added to 10 μg HDL_3, and the protein mixture was digested with trypsin. The peptide digest was then analyzed with SRM on a Thermo TSQ triple quadrupole mass spectrometer. *A*, shown are ion chromatograms of precursor and chlorinated, unlabeled, and ^{15}N-labeled peptides (LAEYHAK) containing Tyr-192. *B*, four transitions (b_2, y_4, y_5, and y_6) were selected to quantify the precursor and chlorinated, unlabeled, and ^{15}N-labeled product peptides (Isqb]LAE*Y*^{192}HAK + H]$^+$ (*m/z* 831.4), [LAE(Cl*Y*^{192})HAK + H]$^+$ (*m/z* 865.4), [^{15}N][LAE*Y*^{192}HAK + H]$^+$ (*m/z* 841.4), and [^{15}N][LAE(Cl*Y*^{192})HAK + H]$^+$ (*m/z* 875.4)]. *RT*, retention time (min).

determine the relative concentrations of chlorinated and nitrated Tyr-containing [^{15}N]peptides. This approach demonstrated excellent linearity ($R > 0.99$) for both 3-chloro-Tyr and 3-nitro-Tyr over a wide range of concentrations (from 1–440 or 0.3–533 pmol/mg HDL protein for 3-chloro-Tyr-192 or 3-nitro-Tyr-192, respectively). Using the method of standard additions and SRM, we estimated that the limits of detection of chlorinated and nitrated Tyr-192 in apoA-I were 0.1 and 0.07 pmol/mg HDL protein, respectively. Similar results were obtained for the other six chlorinated and nitrated tyrosine containing peptides of apoA-I (data not shown). Collectively, these observations indicate that SRM with isotope dilution is a sensitive method for quantifying the regiospecific oxidation of apoA-I.

In Both Lipid-free and HDL-associated apoA-I, Tyr-192 Is Major Target for Chlorination by Reagent HOCl and MPO System—To determine the major site(s) of chlorination of apoA-I *in vitro*, we exposed lipid-free or HDL-associated apolipoprotein (5 μM) to HOCl or the MPO-H_2O_2-chloride system at a 10:1 ratio of oxidant (mol/mol, oxidant:apoA-I) for 60 min at 37 °C. We terminated the reaction with 5 mM methionine and added oxidized [^{15}N]apoA-I. After digesting the proteins with trypsin or Glu-C, we analyzed the resulting peptides with SRM using nano-LC-MS/MS. We then quantified the product yields of 3-chlorotyrosine using the ratio of peak area of the ion current of chlorinated peptides to the total peak area of native and chlorinated peptides. This approach confirmed that Tyr-192 was the predominant site of chlorination (~10%) in both lipid-free (Fig. 2*A*; $p = 0.02$ *versus* Tyr-236, Student's *t* test) and HDL-associated (Fig. 2*B*; $p = 0.01$ *versus* Tyr-115 or Tyr-236) apoA-I when we used either HOCl (Fig. 2; *striped bars*) or the MPO-H_2O_2-chloride system (Fig. 2; *solid bars*). Tyr-115 and Tyr-236 were chlorinated in lower yields (~3–4%; Fig. 2) as were Tyr-18, Tyr-29, Tyr-100, and Tyr-166 (<2%). The product yields for tyrosine chlorination by HOCl and the enzymatic MPO system were similar (compare Fig. 2, *A* and *B*). These findings indicate that Tyr-192 in peptide LAE*Y*HAK is the major site of stable chlorination when apoA-I in its lipid-free or HDL-associated state is exposed to either reagent HOCl or the MPO-H_2O_2-chloride system. They are also consistent with our previous observation that Tyr-192 is the major chlorination site when apoA-I is exposed to MPO (19, 20, 42, 64).

Lipid-free and HDL-associated ApoA-I Exhibit Distinct Patterns of Regiospecific Tyrosine Nitration by ONOO$^-$ and MPO—SRM revealed that when lipid-free apoA-I was exposed to reagent ONOO$^-$ (Fig. 3*A*) or the MPO-H_2O_2-nitrite system (Fig. 3*B*), the predominant tyrosine nitration site was Tyr-192 ($p = 0.02$ *versus* Tyr-100 for ONOO$^-$ and $p = 0.049$ *versus* Tyr-115 for MPO-system, respectively). At a 10:1 molar ratio of oxidant, ~50% of Tyr-192 was nitrated by ONOO$^-$, and ~20% was

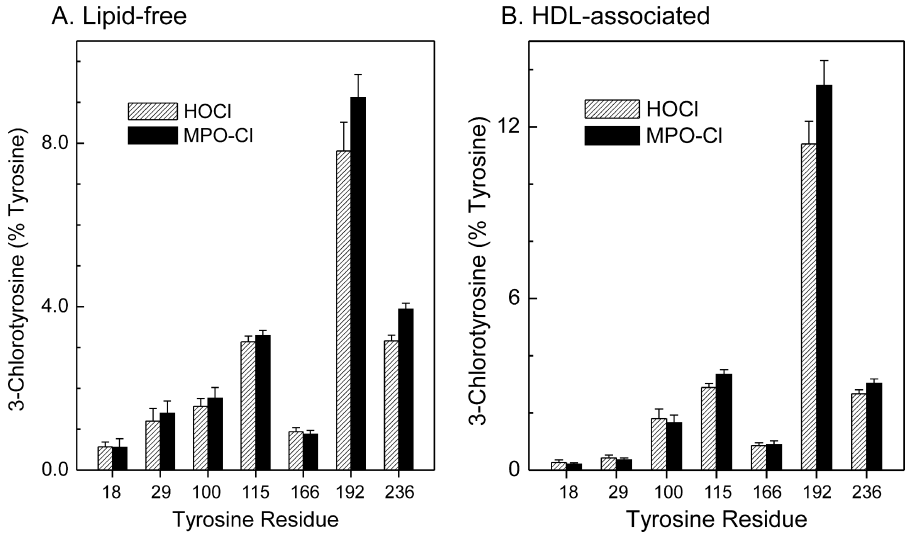

FIGURE 2. **Quantification of regiospecific chlorination of the Tyr residue in lipid-free and HDL-associated apoA-I exposed to HOCl or the MPO-H_2O_2-NaCl system.** Lipid-free apoA-I (10 μM) (*A*) or HDL_3 (0.5 mg/ml, ~12.5 μM apoA-I) (*B*) was exposed to 100 or 180 μM HOCl, respectively (*striped bars*) or to 100 or 180 μM H_2O_2, respectively, in the MPO-H_2O_2-chloride system (*solid bars*) for 60 min at 37 °C in phosphate buffer (20 mM sodium phosphate, 100 μM DTPA, pH 7.4). The MPO system contained 100 nM enzyme and 100 mM sodium chloride. The reaction was terminated with L-methionine. A tryptic digest of apoA-I or HDL_3 was analyzed by selected reaction monitoring mass spectrometry analysis. Four transitions were selected for each Tyr-containing precursor and product peptide to quantify the product yield of chlorinated tyrosine residues. The product yield of 3-chlorotyrosine was calculated as described under "Experimental Procedures." Results are the means ± S.D. of three independent experiments, with triplicate determinations per experiment.

nitrated by MPO. A much lower level (<10%) of nitration was observed at the other tyrosine residues (Fig. 3, *A* and *B*). Reagent $ONOO^-$ was a more selective nitrating agent than the MPO-H_2O_2-nitrite system (Fig. 3). These findings indicate that the predominant nitration site in lipid-free apoA-I by either source of reactive nitrogen species is Tyr-192 (20, 64).

When HDL-associated apoA-I was exposed to reagent $ONOO^-$, SRM demonstrated that Tyr-192 was also the major site of nitration (Fig. 3*C*) ($p = 0.02$ *versus* Tyr-18). At a 10:1 molar ratio of $ONOO^-$, the product yield of nitrated Tyr-192 in lipidated apoA-I was only ⅓ that of lipid-free apoA-I (~15% *versus* ~50%; compare Fig. 3, *A* with *C*). Moreover, the relative nitration level of Tyr-192 decreased (Fig. 3*C*), suggesting that nitration of tyrosine residues in HDL-associated apoA-I by $ONOO^-$ was less selective than when apoA-I was lipid-free.

We observed a different nitration pattern when we exposed HDL-associated apoA-I to the MPO-H_2O_2-nitrite system. Under these conditions, the nitration level of lipid-associated apoA-I was 10-fold lower than when it was lipid-free (compare Fig. 3, *B* and *D*). Moreover, all of the residues were nitrated with approximately the same yield (Fig. 3*B*). These observations suggest that lipid association significantly diminishes the nitration of Tyr residues in apoA-I by both peroxynitrite and the MPO-nitrite system.

Tyrosine 192 Is Major Target for Chlorination and Nitration in ApoA-I of HDL Isolated from Human Plasma—To determine whether specific sites on apoA-I are chlorinated or nitrated *in vivo*, we isolated HDL from human plasma by sequential density gradient ultracentrifugation. To prevent artifactual oxidation, we used buffers containing high concentrations of DTPA (a metal chelator) and butylated hydroxytoluene (a lipid-soluble antioxidant). To quantify the oxidation sites, we supplemented the HDL with oxidized [^{15}N]apoA-I before digesting the proteins with trypsin or Glu-C. We then analyzed the peptic digest with nano-LC-MS/MS and SRM. The modified tyrosine-containing peptides of apoA-I in HDL isolated from humans had the same retention times as the ^{15}N-labeled peptides from [^{15}N]apoA-I oxidized *in vitro* (Table 2). To further confirm the identification of the oxidized peptides, we demonstrated that the MS/MS spectra of the endogenous and corresponding ^{15}N-labeled peptides of apoA-I were virtually identical. The relative amounts of 3-chlorotyrosine and 3-nitrotyrosine were quantified by SRM and comparison of the peak areas of the oxidized ^{15}N-labeled peptides and corresponding endogenous peptides. This approach demonstrated that chlorinated and nitrated peptides were readily detectable in proteolytic digests of apoA-I of HDL isolated from human plasma.

We used nano-LC-MS/MS with SRM and isotope dilution to quantify the sites at which Tyr residues in apoA-I of plasma HDL were modified. These studies identified Tyr-192 as the major target for chlorination (Fig. 4*A*; $n = 11$ healthy subjects) ($p < 0.001$ *versus* Tyr-18). The average level of 3-chlorotyrosine at Tyr-192 was 43 μmol/mol Tyr (Fig. 4*A*). Unexpectedly, we also identified Tyr-18 as a second major site of chlorination in plasma HDL, with an average level of 11 μmol/mol Tyr (Fig. 4*A*). 3-Chlorotyrosine at other tyrosine residues was detected at a lower level (<6 μmol/mol Tyr).

Using the same approach, we found that the average level of 3-nitrotyrosine at Tyr-192 was 45 μmol/mol Tyr in apoA-I of plasma HDL (Fig. 4*B*). Lower levels of 3-nitrotyrosine were detected at other positions. The levels of nitration of Tyr-18 and Tyr-236 were significantly lower than that of Tyr-192 ($p = 0.04$ *versus* Tyr-18 and $p = 0.02$ *versus* Tyr-236). These observations demonstrate that Tyr-192 is the major site for both chlorination and nitration in apoA-I of HDL isolated by ultracentrifugation from plasma of apparently healthy human subjects.

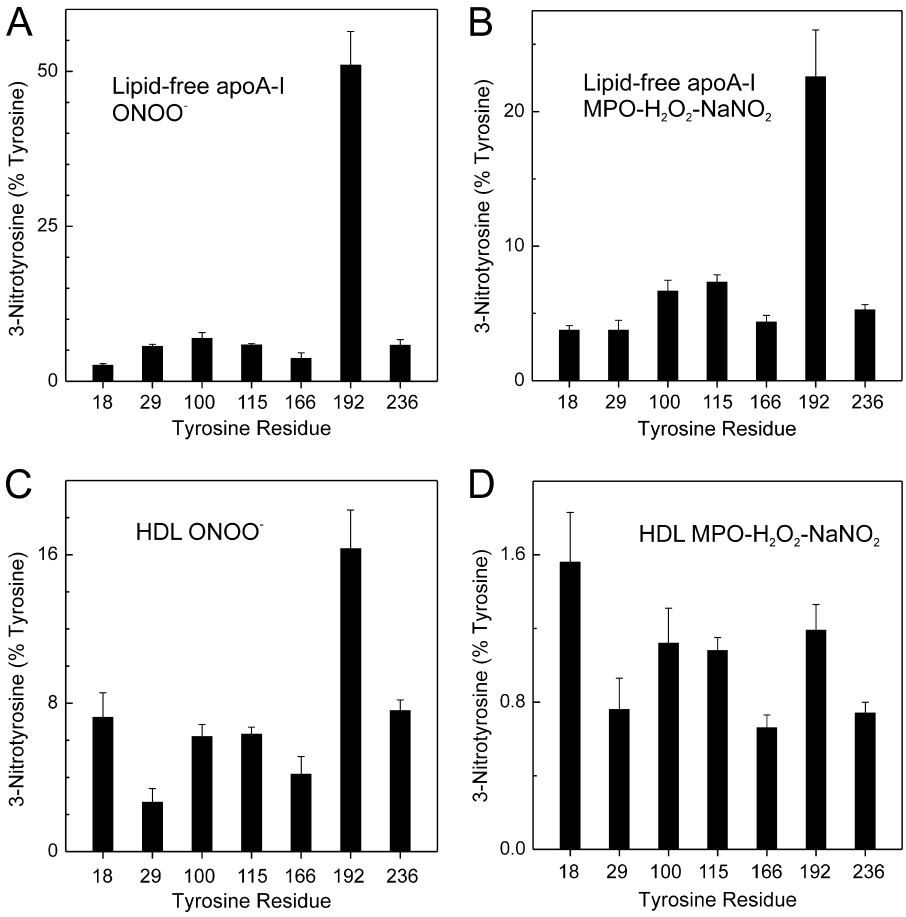

FIGURE 3. **On exposure to the MPO-H_2O_2-$NaNO_2$ system, Tyr-192 is the major nitration target in apoA-I, but Tyr-18 is the major target when apoA-I is associated with HDL.** Lipid-free apoA-I (10 μM) (*A* and *B*) or HDL_3 (0.5 mg/ml, ~12.5 μM apoA-I) (*C* and *D*) was exposed to 100 or 180 μM $ONOO^-$, respectively (*A* and *C*), or to 100 or 180 μM H_2O_2, respectively, in the MPO-H_2O_2-nitrite system (*B* and *D*) for 60 min at 37 °C in phosphate buffer (20 mM sodium phosphate, 100 μM DTPA, pH 7.4). The MPO system was supplemented with 100 nM enzyme and 200 μM sodium nitrite. The reaction was terminated with L-methionine. A tryptic digest of apoA-I or HDL_3 was analyzed by isotope dilution SRM. Four transitions were selected for each Tyr-containing precursor and product peptide to quantify the product yields of nitrated tyrosine residues. Product yield of 3-nitrotyrosine was calculated as described under "Experimental Procedures." Results are the means ± S.D. from three independent experiments.

Tyrosines 192 Is Major Target for Chlorination, but Not Nitration, in HDL Isolated from Human Atherosclerotic Lesions—To determine the chlorination and nitration patterns of tyrosine residues of apoA-I in human atherosclerotic tissue, we isolated HDL by sequential density gradient ultracentrifugation from occlusive carotid atherosclerotic lesions recovered at surgery. Immunoblotting with a monospecific rabbit antibody demonstrated that apoA-I accounted for >50% of the protein in lesion HDL. After digesting HDL with trypsin or Glu-C, we used nano-LC-MS/MS and SRM with oxidized [^{15}N]apoA-I to quantify peptides of apoA-I that contained tyrosine. This approach identified Tyr-192 in apoA-I as the major target for chlorination in lesion HDL (Fig. 5*A*) ($p = 0.03$ *versus* Tyr-18). The average level of 3-chlorotyrosine at Tyr-192 was 199 μmol/mol Tyr in lesion HDL isolated from 8 atherosclerotic lesions from different individuals (Fig. 5*A*). We identified Tyr-18 as the second major site of chlorination in lesion HDL (51 μmol/mol Tyr). 3-Chlorotyrosine at other tyrosine residues was detected at a much lower level (<14 μmol/mol of Tyr). Our observations suggest that Tyr-192 is the major chlorination site in apoA-I from human atherosclerotic tissue, as it is in plasma HDL.

We used the same approach to quantify levels of 3-nitrotyrosine in apoA-I harvested from carotid atherosclerotic lesions. SRM with isotope-labeled internal standard revealed that Tyr-18 exhibited the highest level of nitration, but this did not differ significantly from the level of nitration at Tyr-100 ($p = 0.2$). Moreover, the protein C terminus was nitrated at a lower level than its N terminus. For example, we observed 185, 91, and 65 μmol nitro-Tyr/mol Tyr at Tyr-166, Tyr-192, and Tyr-236, respectively (Fig. 5*B*). In contrast, Tyr-18, Tyr-100, and Tyr-115 were nitrated at 560, 353, and 277 μmol/mol Tyr, respectively (Fig. 5*B*). Tyr-29 is an exception, with an average level of 162 μmol nitro-Tyr/mol Tyr. It is noteworthy that this nitration pattern is similar to the one we observed when we nitrated HDL-associated apoA-I with the MPO-H_2O_2-nitrite system (compare Fig. 5*B* with Fig. 3*D*).

Total 3-Chlorotyrosine and 3-Nitrotyrosine Are Elevated in HDL Isolated from Human Atherosclerotic Lesions—Previous studies using GC-MS or LC-ESI-MS have shown that total levels of 3-chlorotyrosine and 3-nitrotyrosine are higher in lesion HDL than in plasma HDL (19, 21, 41). However, those studies reported total levels of modified residues associated with all HDL proteins. To determine how levels of 3-chlorotyrosine and 3-nitrotyrosine in apoA-I of lesion HDL compare with those in circulating HDL, we calculated the overall levels of Tyr chlorination and nitration for all seven Tyr residues in apoA-I (Fig. 6).

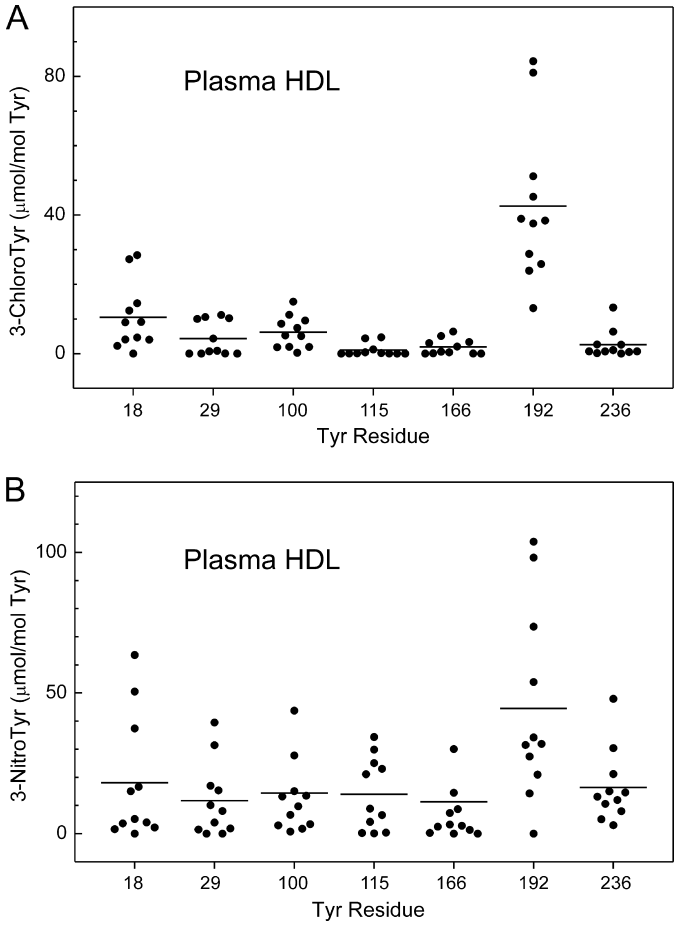

FIGURE 4. **Quantification of the regiospecific chlorination and nitration of apoA-I in HDL isolated from human plasma.** HDL was isolated by ultracentrifugation from plasma of apparently healthy subjects ($n = 11$). An extensively dialyzed mixture of HOCl-chlorinated and peroxynitrite-nitrated [^{15}N]apoA-I (0.15 μg) was added to 10 μg of HDL before digestion. Levels of modified peptides were calculated from the ratio of the total peak area of four transitions of oxidized peptide of apoA-I from HDL relative to that of the corresponding modified [^{15}N]peptides from oxidized [^{15}N]apoA-I as described under "Experimental Procedures." Chlorinated and nitrated tyrosine-containing peptides in the oxidized [^{15}N]apoA-I standards were quantified by LC-ESI-MS-SRM analysis using reconstructed ion chromatograms of product and precursor peptides. Results are representative of those from two independent experiments.

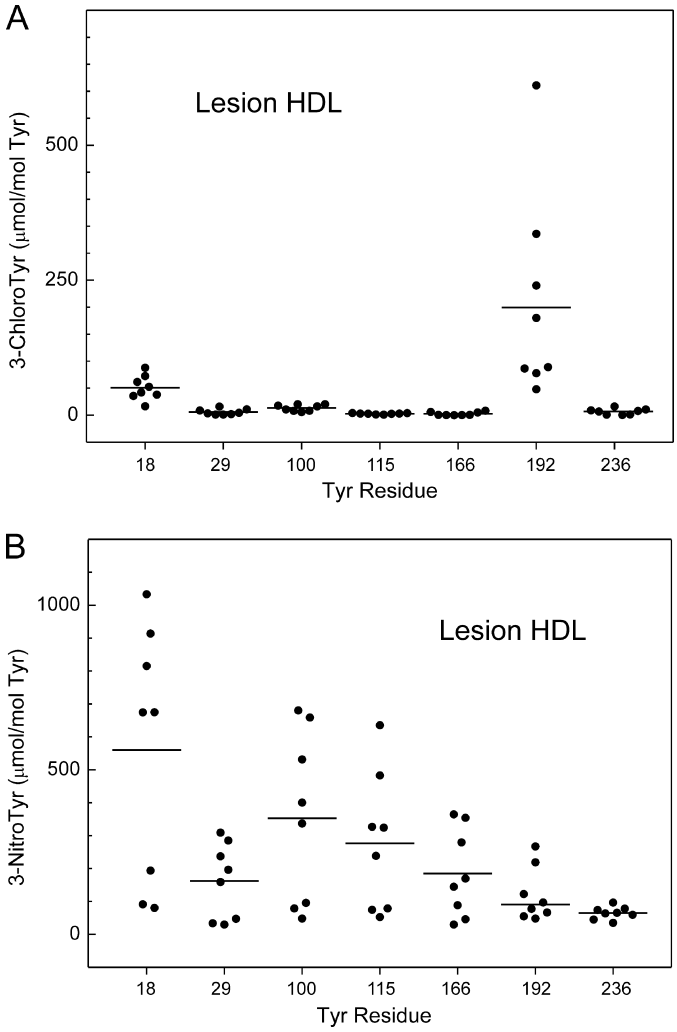

FIGURE 5. **Tyr-192 is the major chlorination target, whereas Tyr-18 is the major nitration target in HDL isolated from human atherosclerotic lesions.** HDL was isolated by ultracentrifugation from atherosclerotic lesions of carotid arteries harvested from humans ($n = 8$). Regiospecific oxidation of apoA-I was determined in tryptic and Glu-C digests of HDL, as described in the legends to Fig. 4. Results are representative of those from two independent experiments.

In lesion HDL, the total level of protein-bound 3-chlorotyrosine (40 ± 24 μmol/mol Tyr; $n = 8$) was 4-fold higher than in circulating HDL (10 ± 3.8 μmol/mol Tyr; $n = 11$) isolated from humans ($p = 0.009$) (Fig. 6*A*). Levels of tyrosine chlorination in lesion HDL ranged from 19 to 89 μmol/mol Tyr, whereas levels of 3-chlorotyrosine in plasma HDL ranged from 6.6 to 19 μmol/mol Tyr.

We also quantified 3-nitrotyrosine. The total level of protein-bound 3-nitrotyrosine in HDL isolated from human aortic atherosclerotic intima (242 ± 160 μmol/mol Tyr; $n = 8$) was 13-fold higher than that in circulating HDL (19 ± 13 μmol/mol Tyr; $n = 11$) isolated from humans ($p = 0.006$) (Fig. 6*B*). Levels of tyrosine nitration in lesion HDL ranged from 45 to 451 μmol/mol Tyr, whereas they ranged from 3.1 to 48 μmol/mol Tyr in plasma HDL. These observations, which agree well with those previously reported for total HDL proteins (19, 21, 41), provide strong evidence that apoA-I of HDL is a major target for damage by MPO and reactive nitrogen intermediates in the human artery wall.

Levels of 3-chloro-Tyr-192 Correlate Strongly with Those of 3-Nitro-Tyr-192 in Both Circulating and Lesion HDL—Studies of MPO-deficient mice strongly suggest that the enzyme is the only source of 3-chlorotyrosine during acute inflammation (30). However, both MPO-dependent and -independent pathways generate 3-nitrotyrosine in these animals (34). To determine whether MPO might promote protein nitration in humans, we assessed the relationship between levels of 3-chlorotyrosine and 3-nitrotyrosine at Tyr-192, the major site of chlorination in both circulating and lesion HDL and the major site of nitration in plasma HDL. Linear regression analysis demonstrated a strong correlation in both plasma HDL ($R^2 = 0.51$; $p = 0.01$, Fig. 7*A*) and lesion HDL ($R^2 = 0.74$; $p = 0.006$, Fig. 7*B*). Moreover, Tyr-18 of apoA-I was the major site of nitration in HDL exposed to the MPO-H_2O_2-nitrite system (Fig. 3*D*), and Tyr-18 was the major site of nitration in lesion HDL (Fig. 5*B*),

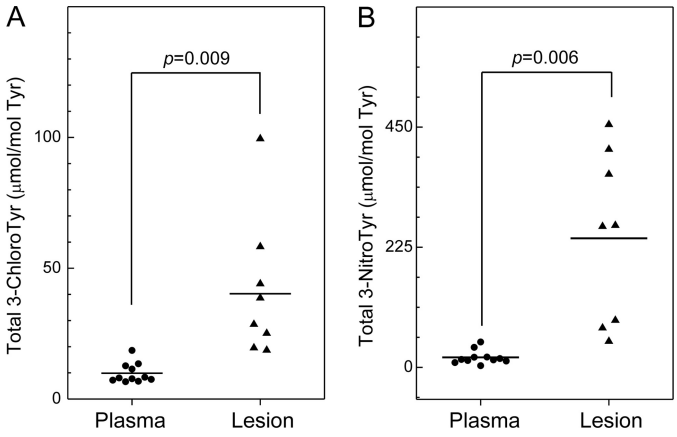

FIGURE 6. **Total levels of 3-chlorotyrosine and 3-nitrotyrosine in apoA-I of HDL isolated from human plasma and atherosclerotic carotid lesions.** HDL was isolated from plasma and atherosclerotic tissue by sequential ultracentrifugation. Levels of individual 3-chlorotyrosine and 3-nitrotyrosine were quantified as described in the legends of Figs. 4 and 5. Total levels of 3-chlorotyrosine or 3-nitrotyrosine in apoA-I were calculated as the sum of individual levels of 3-chlorotyrosine or 3-nitrotyrosine at the 7 Tyr residues in apoA-I divided by 7. Results are representative of those from two independent experiments.

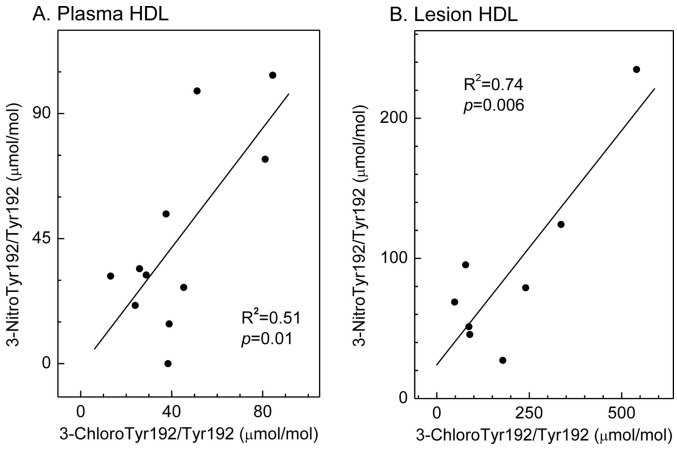

FIGURE 7. **Correlation of 3-chlorotyrosine with 3-nitrotyrosine levels in apoA-I of HDL isolated from human plasma and atherosclerotic lesions.** Levels of 3-chlorotyrosine and 3-nitrotyrosine at Tyr-192 in apoA-I of HDL isolated from plasma (*A*) or lesions (*B*) were determined as described in the legends of Figs. 4 and 5. The coefficient of determination (R^2) and *p* value were calculated by linear regression analysis.

further supporting the proposal that MPO is the major pathway for chlorination and nitration of HDL in human atherosclerotic tissue.

DISCUSSION

Using a sensitive and quantitative SRM-based approach, we demonstrated that Tyr-192 is the major chlorination site in apoA-I of HDL isolated from human atherosclerotic tissue. We obtained the same result with plasma HDL. Moreover, we found elevated levels of 3-chlorotyrosine in apoA-I of lesion HDL, consistent with previous reports that 3-chlorotyrosine levels in the total proteins of lesion HDL are markedly higher than in plasma HDL (19, 21, 41).

Chlorination of Tyr-192 together with methionine oxidation in lipid-free apoA-I by MPO impairs the apolipoprotein ability to promote cholesterol efflux from cells by the ABCA1 pathway (40). Our observations support the proposal that regiospecific chlorination of Tyr-192 of apoA-I by MPO might contribute to the generation of dysfunctional form of HDL in the human artery wall (15). It is therefore possible that modified forms of apoA-I that are resistant to oxidation might be cardioprotective *in vivo*.

The regiospecific patterns of nitration and chlorination of Tyr residues in apoA-I of HDL were different. As with chlorination of lesion HDL, SRM demonstrated that Tyr-192 was the major site of nitration in apoA-I in plasma HDL. In contrast, there was a non-significant trend toward higher levels of nitration of Tyr-18 in apoA-I of lesion HDL. As with 3-chlorotyrosine, the level of total 3-nitrotyrosine in apoA-I of lesion HDL was higher than in circulating HDL. Interestingly, the nitration pattern of plasma HDL was similar to that of HDL-associated apoA-I exposed to $ONOO^-$ *in vitro*. However, the nitration pattern of lesion HDL was similar to that of HDL-associated apoA-I exposed to the MPO-H_2O_2-nitrite system. These observations suggest that MPO is the major pathway for nitrating HDL in human atherosclerotic tissue, whereas both the $ONOO^-$ and MPO pathways (and perhaps other sources of reactive nitrogen species) help generate the nitrated HDL that ultimately appears in plasma.

MPO is the only known source of 3-chlorotyrosine *in vivo* (30). Therefore, a strong correlation between levels of 3-chlorotyrosine and 3-nitrotyrosine in apoA-I would support the proposal that MPO is the major pathway for nitrating HDL *in vivo*. Indeed, we observed a strong relationship, as assessed by linear regression ($R^2 = 0.74$), between chlorination and nitration levels at residues Tyr-192 of apoA-I in lesion HDL. This relationship was weaker ($R^2 = 0.51$) for plasma HDL, consistent with the proposal that pathways distinct from MPO contribute to HDL nitration in plasma.

A key question is why Tyr-192 is so much more amenable to chlorination and nitration than the six other tyrosine residues in apoA-I. We previously used electron paramagnetic resonance spectroscopy and lipid-free spin-labeled apoA-I to demonstrate that the side chain of Tyr-192 resides in a hydrophilic environment that assumes a random coil conformation (20). When apoA-I is associated with lipid in a discoidal particle (68), Tyr-192 partitions into a much more hydrophobic environment, likely at the complex lipid-water interface. The secondary structure of this region of apoA-I also undergoes a transition to an amphipathic α-helix (68). These observations indicate that lipid association markedly affects the environment of residue 192, strongly suggesting that Tyr-192 in lipid-free apoA-I is readily accessible to aqueous solvent.

Both $ONOO^-$ and $NO_2^{\bullet}$, the proposed product of nitrite oxidation by MPO, are strong oxidizing intermediates that rapidly react with biomolecules (39, 69). Both reactive intermediates are generated in aqueous environments, suggesting that they will initially encounter functional groups that are also in the aqueous milieu. Consistent with its accessibility to solvent, Tyr-192 in lipid-free apoA-I was the major nitration site for both MPO and $ONOO^-$. However, when apoA-I was incorporated into HDL particles, nitration of Tyr-192 was markedly reduced. Moreover, the product yields of 3-nitrotyrosine were strikingly lower when apoA-I was associated with HDL than when it was lipid-free. These observations suggest that when

apoA-I is associated with HDL, Tyr-192 partitions into a more hydrophobic environment and is, therefore, unable to react with nitrating intermediates generated in the aqueous phase by MPO and $ONOO^-$. Thus, accessibility to solvent is likely to be an important feature controlling the nitration of Tyr-192 in apoA-I both in the lipid-free and HDL-associated states (20, 39, 49, 70).

Two models have been proposed for the site-specific chlorination of apoA-I by MPO (21, 42). The first centers on the reaction of HOCl with the side chain (an amino group) of lysines to form chloramines, which promote tyrosine chlorination (28, 42). Tyr-192 lies two residues away from Lys-195 in a sequence we have termed the Y*XX*K motif. Studies with synthetic peptides (42) and mutations of apoA-I provided strong evidence that the Y*XX*K/K*XX*Y motif (40) can direct the regiospecific chlorination of tyrosine residues.

Zheng *et al.* (21) proposed a different model for site-specific chlorination. Using hydrogen-deuterium exchange, they found that MPO interacts with the region of apoA-I that contains Tyr-192. Based on these results, they proposed that MPO promotes site-specific chlorination when it binds directly to the region of apoA-I that contains Tyr-192.

To distinguish between these models, we exposed lipid-free or HDL-associated apoA-I to reagent HOCl or the complete MPO-H_2O_2-chloride system and analyzed the reaction products by SRM. The pattern of tyrosine chlorination in apoA-I by HOCl was virtually identical to that with the enzymatic system with either lipid-free or HDL-associated apoA-I. These results provide strong evidence that reagent HOCl promotes the regiospecific chlorination of tyrosine residues, a system that clearly cannot involve direct interaction of MPO with apoA-I.

In contrast to its behavior with reactive nitrogen species, Tyr-192 was chlorinated in high yield in both lipid-free and HDL-associated apoA-I. This tyrosine resides in a Y*XX*K motif. We previously showed that HOCl reacts with lysine residues in peptides to form long-lived chloramines that promote the regiospecific chlorination of tyrosine (42). In contrast to the free N^{ϵ} amino group of lysine ($pK_a \sim 10.5$), which exists predominantly as the protonated NH_3^+ species at neutral pH, the chloramine derived from the lysine N^{ϵ} amino group is uncharged. Thus, this long-lived species could potentially attack the phenol group of tyrosine in either a hydrophilic or hydrophobic environment. Moreover, Tyr-192 lies in an α-helical structure when apoA-I associates with lipid (68), which positions it for interacting with Lys-195. These observations are consistent with our demonstration that Tyr-192 is the major chlorination site in apoA-I *in vivo* and with the proposal that the chloramine of Lys-195 can direct the chlorination of Tyr-192 of apoA-I in high yield in both lipid-free and HDL-associated protein.

Our observations indicate that Tyr-192 of apoA-I is the major chlorination site in HDL isolated from human plasma or atherosclerotic lesions. We have proposed that chlorination is a pericellular process that occurs because activated macrophages use NADPH oxidase to produce high fluxes of H_2O_2 near the plasma membrane. They also secrete MPO, which converts the H_2O_2 to HOCl. The hypohalous acid then modifies specific Tyr-192 and methionine residues in apoA-I.

In summary, we have demonstrated that Tyr-192 is the major site of chlorination in apoA-I of HDL isolated from human atherosclerotic lesions. Oxidation of lipid-free apoA-I inhibits cholesterol efflux by the ABCA1 pathway, whereas damage to lipid-associated apoA-I impairs lecithin:cholesterol acyltransferase activation. Thus, MPO inhibits two key early steps in cholesterol efflux from macrophages by modifying specific Tyr and methionine residues in apoA-I. These observations support the proposal that oxidation-resistant forms of apoA-I might be cardioprotective in the artery wall of humans. They further suggest that quantifying apoA-I chlorination might help diagnose and perhaps treat human cardiovascular disease.

Acknowledgment—Mass spectrometry experiments were performed by the Proteomics Core, the Diabetes Education and Research Center, University of Washington (P30DK017047).

REFERENCES

1. Gordon, D. J., and Rifkind, B. M. (1989) High density lipoprotein. The clinical implications of recent studies. *N. Engl. J. Med.* **321,** 1311–1316
2. Movva, R., and Rader, D. J. (2008) Laboratory assessment of HDL heterogeneity and function. *Clin Chem.* **54,** 788–800
3. Oram, J. F., and Heinecke, J. W. (2005) ATP binding cassette transporter A1. A cell cholesterol exporter that protects against cardiovascular disease. *Physiol. Rev.* **85,** 1343–1372
4. Rothblat, G. H., and Phillips, M. C. (2010) High density lipoprotein heterogeneity and function in reverse cholesterol transport. *Curr. Opin. Lipidol.* **21,** 229–238
5. Yvan-Charvet, L., Wang, N., and Tall, A. R. (2010) Role of HDL, ABCA1, and ABCG1 transporters in cholesterol efflux and immune responses. *Arterioscler. Thromb. Vasc. Biol.* **30,** 139–143
6. Aiello, R. J., Brees, D., Bourassa, P. A., Royer, L., Lindsey, S., Coskran, T., Haghpassand, M., and Francone, O. L. (2002) Increased atherosclerosis in hyperlipidemic mice with inactivation of ABCA1 in macrophages. *Arterioscler. Thromb. Vasc. Biol.* **22,** 630–637
7. Out, R., Hoekstra, M., Habets, K., Meurs, I., de Waard, V., Hildebrand, R. B., Wang, Y., Chimini, G., Kuiper, J., Van Berkel, T. J., and Van Eck, M. (2008) Combined deletion of macrophage ABCA1 and ABCG1 leads to massive lipid accumulation in tissue macrophages and distinct atherosclerosis at relatively low plasma cholesterol levels. *Arterioscler. Thromb. Vasc. Biol.* **28,** 258–264
8. Yvan-Charvet, L., Ranalletta, M., Wang, N., Han, S., Terasaka, N., Li, R., Welch, C., and Tall, A. R. (2007) Combined deficiency of ABCA1 and ABCG1 promotes foam cell accumulation and accelerates atherosclerosis in mice. *J. Clin. Invest.* **117,** 3900–3908
9. Brunham, L. R., Singaraja, R. R., Duong, M., Timmins, J. M., Fievet, C., Bissada, N., Kang, M. H., Samra, A., Fruchart, J. C., McManus, B., Staels, B., Parks, J. S., and Hayden, M. R. (2009) Tissue-specific roles of ABCA1 influence susceptibility to atherosclerosis. *Arterioscler. Thromb. Vasc. Biol.* **29,** 548–554
10. Van Eck, M., Singaraja, R. R., Ye, D., Hildebrand, R. B., James, E. R., Hayden, M. R., and Van Berkel, T. J. (2006) Macrophage ATP binding cassette transporter A1 overexpression inhibits atherosclerotic lesion progression in low density lipoprotein receptor knockout mice. *Arterioscler. Thromb. Vasc. Biol.* **26,** 929–934
11. Glomset, J. A. (1968) The plasma lecithins. Cholesterol acyltransferase reaction. *J. Lipid Res.* **9,** 155–167
12. Jonas, A. (1991) Lecithin-cholesterol acyltransferase in the metabolism of high density lipoproteins. *Biochim Biophys Acta* **1084,** 205–220
13. Vaughan, A. M., and Oram, J. F. (2006) ABCA1 and ABCG1 or ABCG4 act sequentially to remove cellular cholesterol and generate cholesterol-rich HDL. *J. Lipid Res.* **47,** 2433–2443
14. Barter, P. J., Nicholls, S., Rye, K. A., Anantharamaiah, G. M., Navab, M., and Fogelman, A. M. (2004) Antiinflammatory properties of HDL. *Circ.*

Res. **95,** 764–772
15. Shao, B., Oda, M. N., Oram, J. F., and Heinecke, J. W. *Chem. Res. Toxicol.* **23,** 447–454
16. Ory, D. S., and Schaffer, J. E. (2010) ApoA-1 in diabetes: damaged goods. *Diabetes.* **59,** 2358–2359
17. Francis, G. A. (2010) The complexity of HDL. *Biochim. Biophys. Acta* **1801,** 1286–1293
18. Daugherty, A., Dunn, J. L., Rateri, D. L., and Heinecke, J. W. (1994) Myeloperoxidase, a catalyst for lipoprotein oxidation, is expressed in human atherosclerotic lesions. *J. Clin. Invest.* **94,** 437–444
19. Bergt, C., Pennathur, S., Fu, X., Byun, J., O'Brien, K., McDonald, T. O., Singh, P., Anantharamaiah, G. M., Chait, A., Brunzell, J., Geary, R. L., Oram, J. F., and Heinecke, J. W. (2004) The myeloperoxidase product hypochlorous acid oxidizes HDL in the human artery wall and impairs ABCA1-dependent cholesterol transport. *Proc. Natl. Acad. Sci. U.S.A.* **101,** 13032–13037
20. Shao, B., Bergt, C., Fu, X., Green, P., Voss, J. C., Oda, M. N., Oram, J. F., and Heinecke, J. W. (2005) Tyrosine 192 in apolipoprotein A-I is the major site of nitration and chlorination by myeloperoxidase, but only chlorination markedly impairs ABCA1-dependent cholesterol transport. *J. Biol. Chem.* **280,** 5983–5993
21. Zheng, L., Nukuna, B., Brennan, M. L., Sun, M., Goormastic, M., Settle, M., Schmitt, D., Fu, X., Thomson, L., Fox, P. L., Ischiropoulos, H., Smith, J. D., Kinter, M., and Hazen, S. L. (2004) Apolipoprotein A-I is a selective target for myeloperoxidase-catalyzed oxidation and functional impairment in subjects with cardiovascular disease. *J. Clin. Invest.* **114,** 529–541
22. Shao, B., Cavigiolio, G., Brot, N., Oda, M. N., and Heinecke, J. W. (2008) Methionine oxidation impairs reverse cholesterol transport by apolipoprotein A-I. *Proc. Natl. Acad. Sci. U.S.A.* **105,** 12224–12229
23. Wu, Z., Wagner, M. A., Zheng, L., Parks, J. S., Shy, J. M., 3rd, Smith, J. D., Gogonea, V., and Hazen, S. L. (2007) The refined structure of nascent HDL reveals a key functional domain for particle maturation and dysfunction. *Nat. Struct. Mol. Biol.* **14,** 861–868
24. Gordon, S. M., Hofmann, S., Askew, D. S., and Davidson, W. S. (2011) High density lipoprotein. It Is not just about lipid transport anymore. *Trends Endocrinol. Metab.* **22,** 9–15
25. Winterbourn, C. C., and Kettle, A. J. (2000) Biomarkers of myeloperoxidase-derived hypochlorous acid. *Free Radic. Biol. Med.* **29,** 403–409
26. Klebanoff, S. J. (1999) Myeloperoxidase. *Proc. Assoc. Am. Physicians* **111,** 383–389
27. Jiang, Q., Griffin, D. A., Barofsky, D. F., and Hurst, J. K. (1997) Intraphagosomal chlorination dynamics and yields determined using unique fluorescent bacterial mimics. *Chem. Res. Toxicol.* **10,** 1080–1089
28. Domigan, N. M., Charlton, T. S., Duncan, M. W., Winterbourn, C. C., and Kettle, A. J. (1995) Chlorination of tyrosyl residues in peptides by myeloperoxidase and human neutrophils. *J. Biol. Chem.* **270,** 16542–16548
29. Hazen, S. L., Hsu, F. F., Mueller, D. M., Crowley, J. R., and Heinecke, J. W. (1996) Human neutrophils employ chlorine gas as an oxidant during phagocytosis. *J. Clin. Invest.* **98,** 1283–1289
30. Gaut, J. P., Yeh, G. C., Tran, H. D., Byun, J., Henderson, J. P., Richter, G. M., Brennan, M. L., Lusis, A. J., Belaaouaj, A., Hotchkiss, R. S., and Heinecke, J. W. (2001) Neutrophils employ the myeloperoxidase system to generate antimicrobial brominating and chlorinating oxidants during sepsis. *Proc. Natl. Acad. Sci. U.S.A.* **98,** 11961–11966
31. Cooper, C. E., Patel, R. P., Brookes, P. S., and Darley-Usmar, V. M. (2002) Nanotransducers in cellular redox signaling. Modification of thiols by reactive oxygen and nitrogen species. *Trends Biochem. Sci.* **27,** 489–492
32. Moncada, S., Palmer, R. M., and Higgs, E. A. (1991) Nitric oxide: physiology, pathophysiology, and pharmacology. *Pharmacol. Rev.* **43,** 109–142
33. Wink, D. A., and Mitchell, J. B. (1998) Chemical biology of nitric oxide. Insights into regulatory, cytotoxic, and cytoprotective mechanisms of nitric oxide. *Free Radic. Biol Med.* **25,** 434–456
34. Beckman, J. S., Chen, J., Ischiropoulos, H., and Crow, J. P. (1994) Oxidative chemistry of peroxynitrite. *Methods Enzymol.* **233,** 229–240
35. Eiserich, J. P., Hristova, M., Cross, C. E., Jones, A. D., Freeman, B. A., Halliwell, B., and van der Vliet, A. (1998) Formation of nitric oxide-derived inflammatory oxidants by myeloperoxidase in neutrophils. *Nature* **391,** 393–397
36. Gaut, J. P., Byun, J., Tran, H. D., Lauber, W. M., Carroll, J. A., Hotchkiss, R. S., Belaaouaj, A., and Heinecke, J. W. (2002) Myeloperoxidase produces nitrating oxidants *in vivo*. *J. Clin. Invest.* **109,** 1311–1319
37. Carr, A. C., McCall, M. R., and Frei, B. (2000) Oxidation of LDL by myeloperoxidase and reactive nitrogen species. Reaction pathways and antioxidant protection. *Arterioscler. Thromb. Vasc. Biol.* **20,** 1716–1723
38. Klebanoff, S. J. (1993) Reactive nitrogen intermediates and antimicrobial activity. Role of nitrite. *Free Radic. Biol. Med.* **14,** 351–360
39. Radi, R., Peluffo, G., Alvarez, M. N., Naviliat, M., and Cayota, A. (2001) Unraveling peroxynitrite formation in biological systems. *Free Radic. Biol. Med.* **30,** 463–488
40. Shao, B., Oda, M. N., Bergt, C., Fu, X., Green, P. S., Brot, N., Oram, J. F., and Heinecke, J. W. (2006) Myeloperoxidase impairs ABCA1-dependent cholesterol efflux through methionine oxidation and site-specific tyrosine chlorination of apolipoprotein A-I. *J. Biol. Chem.* **281,** 9001–9004
41. Pennathur, S., Bergt, C., Shao, B., Byun, J., Kassim, S. Y., Singh, P., Green, P. S., McDonald, T. O., Brunzell, J., Chait, A., Oram, J. F., O'brien, K., Geary, R. L., and Heinecke, J. W. (2004) Human atherosclerotic intima and blood of patients with established coronary artery disease contain high density lipoprotein damaged by reactive nitrogen species. *J. Biol. Chem.* **279,** 42977–42983
42. Bergt, C., Fu, X., Huq, N. P., Kao, J., and Heinecke, J. W. (2004) Lysine residues direct the chlorination of tyrosines in Y*XX*K motifs of apolipoprotein A-I when hypochlorous acid oxidizes high density lipoprotein. *J. Biol. Chem.* **279,** 7856–7866
43. Zheng, L., Settle, M., Brubaker, G., Schmitt, D., Hazen, S. L., Smith, J. D., and Kinter, M. (2005) Localization of nitration and chlorination sites on apolipoprotein A-I catalyzed by myeloperoxidase in human atheroma and associated oxidative impairment in ABCA1-dependent cholesterol efflux from macrophages. *J. Biol. Chem.* **280,** 38–47
44. Mallick, P., Schirle, M., Chen, S. S., Flory, M. R., Lee, H., Martin, D., Ranish, J., Raught, B., Schmitt, R., Werner, T., Kuster, B., and Aebersold, R. (2007) Computational prediction of proteotypic peptides for quantitative proteomics. *Nat. Biotechnol.* **25,** 125–131
45. Anderson, L., and Hunter, C. L. (2006) Quantitative mass spectrometric multiple reaction monitoring assays for major plasma proteins. *Mol. Cell. Proteomics* **5,** 573–588
46. Gerber, S. A., Rush, J., Stemman, O., Kirschner, M. W., and Gygi, S. P. (2003) Absolute quantification of proteins and phosphoproteins from cell lysates by tandem MS. *Proc. Natl. Acad. Sci. U.S.A.* **100,** 6940–6945
47. Berliner, J. A., and Heinecke, J. W. (1996) The role of oxidized lipoproteins in atherogenesis. *Free Radic. Biol. Med.* **20,** 707–727
48. Heinecke, J. W. (1998) Oxidants and antioxidants in the pathogenesis of atherosclerosis. Implications for the oxidized low density lipoprotein hypothesis. *Atherosclerosis* **141,** 1–15
49. Souza, J. M., Daikhin, E., Yudkoff, M., Raman, C. S., and Ischiropoulos, H. (1999) Factors determining the selectivity of protein tyrosine nitration. *Arch. Biochem. Biophys.* **371,** 169–178
50. Calabresi, L., Sirtori, C. R., Paoletti, R., and Franceschini, G. (2006) Recombinant apolipoprotein A-I Milano for the treatment of cardiovascular diseases. *Curr. Atheroscler. Rep.* **8,** 163–167
51. Chiesa, G., and Sirtori, C. R. (2003) Recombinant apolipoprotein A-I (Milano). A novel agent for the induction of regression of atherosclerotic plaques. *Ann. Med.* **35,** 267–273
52. Nissen, S. E., Tsunoda, T., Tuzcu, E. M., Schoenhagen, P., Cooper, C. J., Yasin, M., Eaton, G. M., Lauer, M. A., Sheldon, W. S., Grines, C. L., Halpern, S., Crowe, T., Blankenship, J. C., and Kerensky, R. (2003) Effect of recombinant apoA-I Milano on coronary atherosclerosis in patients with acute coronary syndromes. A randomized controlled trial. *JAMA* **290,** 2292–2300
53. Heinecke, J. W., Hsu, F. F., Crowley, J. R., Hazen, S. L., Leeuwenburgh, C., Mueller, D. M., Rasmussen, J. E., and Turk, J. (1999) Detecting oxidative modification of biomolecules with isotope dilution mass spectrometry. Sensitive and quantitative assays for oxidized amino acids in proteins and tissues. *Methods Enzymol.* **300,** 124–144
54. Heinecke, J. W., Li, W., Daehnke, H. L., 3rd, and Goldstein, J. A. (1993) Dityrosine, a specific marker of oxidation, is synthesized by the myeloperoxidase-hydrogen peroxide system of human neutrophils and macro-

phages. *J. Biol. Chem.* **268,** 4069–4077
55. Morita, Y., Iwamoto, H., Aibara, S., Kobayashi, T., and Hasegawa, E. (1986) Crystallization and properties of myeloperoxidase from normal human leukocytes. *J. Biochem.* **99,** 761–770
56. Ryan, R. O., Forte, T. M., and Oda, M. N. (2003) Optimized bacterial expression of human apolipoprotein A-I. *Protein Expr. Purif.* **27,** 98–103
57. Mendez, A. J., Oram, J. F., and Bierman, E. L. (1991) Protein kinase C as a mediator of high density lipoprotein receptor-dependent efflux of intracellular cholesterol. *J. Biol. Chem.* **266,** 10104–10111
58. Shao, B., Pennathur, S., Pagani, I., Oda, M. N., Witztum, J. L., Oram, J. F., and Heinecke, J. W. (2010) Modifying apolipoprotein A-I by malondialdehyde, but not by an array of other reactive carbonyls, blocks cholesterol efflux by the ABCA1 pathway. *J. Biol. Chem.* **285,** 18473–18484
59. Heinecke, J. W., Baker, L., Rosen, H., and Chait, A. (1986) Superoxide-mediated modification of low density lipoprotein by arterial smooth muscle cells. *J. Clin. Invest.* **77,** 757–761
60. Heinecke, J. W., Rosen, H., and Chait, A. (1984) Iron and copper promote modification of low density lipoprotein by human arterial smooth muscle cells in culture. *J. Clin. Invest.* **74,** 1890–1894
61. Nelson, D. P., and Kiesow, L. A. (1972) Enthalpy of decomposition of hydrogen peroxide by catalase at 25 °C (with molar extinction coefficients of H_2O_2 solutions in the UV). *Anal. Biochem.* **49,** 474–478
62. Crouch, E. C., Hirche, T. O., Shao, B., Boxio, R., Wartelle, J., Benabid, R., McDonald, B., Heinecke, J., Matalon, S., and Belaaouaj, A. (2010) Myeloperoxidase-dependent inactivation of surfactant protein D *in vitro* and *in vivo*. *J. Biol. Chem.* **285,** 16757–16770
63. Shao, B., Fu, X., McDonald, T. O., Green, P. S., Uchida, K., O'Brien, K. D., Oram, J. F., and Heinecke, J. W. (2005) Acrolein impairs ATP binding cassette transporter A1-dependent cholesterol export from cells through site-specific modification of apolipoprotein A-I. *J. Biol. Chem.* **280,** 36386–36396
64. Shao, B., and Heinecke, J. W. (2008) Using tandem mass spectrometry to quantify site-specific chlorination and nitration of proteins. Model system studies with high density lipoprotein oxidized by myeloperoxidase. *Methods Enzymol.* **440,** 33–63
65. MacLean, B., Tomazela, D. M., Shulman, N., Chambers, M., Finney, G. L., Frewen, B., Kern, R., Tabb, D. L., Liebler, D. C., and MacCoss, M. J. (2010) Skyline. An open source document editor for creating and analyzing targeted proteomics experiments. *Bioinformatics* **26,** 966–968
66. Hunt, S. (1984) Halogenated tyrosine derivatives in invertebrate scleroproteins. Isolation and identification. *Methods Enzymol.* **107,** 413–438
67. Malan, P. G., and Edelhoch, H. (1970) Nitration of human serum albumin and bovine and human goiter thyroglobulins with tetranitromethane. *Biochemistry* **9,** 3205–3214
68. Oda, M. N., Forte, T. M., Ryan, R. O., and Voss, J. C. (2003) The C-terminal domain of apolipoprotein A-I contains a lipid-sensitive conformational trigger. *Nat. Struct. Biol.* **10,** 455–460
69. Kettle, A. J., van Dalen, C. J., and Winterbourn, C. C. (1997) Peroxynitrite and myeloperoxidase leave the same footprint in protein nitration. *Redox Rep.* **3,** 257–258
70. Ischiropoulos, H. (2003) Biological selectivity and functional aspects of protein tyrosine nitration. *Biochem. Biophys. Res. Commun.* **305,** 776–783